Radiation efficiency of a distribution of baffled pistons with arbitrary phases

Carlos García A, Nicolas Dauchez, Gautier Lefebvre

Radiation efficiency of a distribution of baffled pistons with arbitrary phases

Carlos García A., Nicolas Dauchez and Gautier Lefebvre

Citation: The Journal of the Acoustical Society of America **152**, 1135 (2022); doi: 10.1121/10.0013569
View online: https://doi.org/10.1121/10.0013569
View Table of Contents: https://asa.scitation.org/toc/jas/152/2
Published by the Acoustical Society of America

JASA ARTICLE

Radiation efficiency of a distribution of baffled pistons with arbitrary phases

Carlos García A.,[a] Nicolas Dauchez, and Gautier Lefebvre
Université de Technologie de Compiègne, Roberval (Mechanics, Energy and Electricity), Centre de Recherche Royallieu, CS 60319, 60203 Compiègne Cedex, France

ABSTRACT:
The radiation resistance and efficiency of a collection of circular pistons, randomly placed on a plane and vibrating with arbitrary phases, are expressed as a combination of the self- and mutual-radiation components. We use the first product or bridge theorem to construct the directivity pattern of this type of arrangement and the radiation properties are calculated according to Bouwkamp's impedance theorem. To illustrate the versatility of our approach, we refer to special cases for symmetric arrangements, for example, to compare with the modal radiation efficiency in structures having "regular" modal patterns. © *2022 Acoustical Society of America*. https://doi.org/10.1121/10.0013569

(Received 17 May 2022; revised 6 July 2022; accepted 27 July 2022; published online 24 August 2022)
[Editor: Nicole Kessissoglou] Pages: 1135–1145

I. INTRODUCTION

The acoustic radiation impedance of a circular piston is a fundamental problem in acoustics and has been well-documented over the last two centuries. Early studies in optics describing the passage of plane waves through circular apertures (Babinet, 1837) Rayleigh, 1897; and Bouwkamp, 1970) were used later to define the radiation of a baffled piston. The Rayleigh integral (Rayleigh, 1945), as a consequence of these previous studies, has become a widely used tool to express not only the radiation of a circular piston in an infinite baffle but to approximate the radiation of loudspeakers in an enclosure. Special equations describing the force over the surface of the piston were studied by Rayleigh, King (1934), Struve (1882), and Greenspan (1979) who derived a solution of the Hankel transform and obtained the exerted force over the radiator and thus, the acoustic impedance. While the imaginary part of the acoustic impedance, the radiation reactance, creates an evanescent field and does not radiate sound, the radiation resistance is responsible for the radiation of sound into the far-field. The radiation resistance can be obtained by calculating the acoustic source's power by integrating the real part of the intensity over a hemisphere and letting the radius tend to infinity. A generalization of this procedure led later to Bouwkamp's impedance theorem (Bouwkamp, 1945): if the directivity of a source is known, its radiation impedance can be calculated by integrating the squared directivity over a hemisphere. This method was employed to calculate, for example, the radiation impedance of circular, rectangular, elliptic (Mellow and Kärkkäinen, 2016) flat rigid disks.

When two sources are present, the acoustic effect of one source on the other is described by the mutual-radiation impedance. Pritchard (1960) calculated the mutual radiation of two pistons in a series formed by expanding the Bessel functions with Lommel's theorem and identifying specific cases of Sonine integrals. Porter (1964) generalized this method for flexural baffled disks and Chan (1967) extended it for radiators of different sizes. Crane (1967) used the "Gutin" concept to explore the radiation of unbaffled and partially baffled pistons, and Van Buren and King (1973) studied the self- and mutual-impedance of two coplanar unbaffled disks. Stepanishen (1978) used the impulse response method approach to give a simple approximation of the mutual radiation coefficient. This method was later utilized by Hashimoto (2001) to calculate the radiation of a structure in terms of elementary radiators with the acoustic radiation resistance matrix (ARM): a flat structure is decomposed into equally small sections or radiators, each radiator is considered a circular piston and the acoustic impedance of the structure is expressed in a matrix form, taking into account the self- and mutual-radiation impedance. Going further, this semi-analytical formulation was employed by Arenas (2008) for calculating the radiation properties of simple baffled structures in terms of structural and radiation modes (see also Elliott and Johnson, 1993; Naghshineh and Koopmann, 1991). Arenas (2009) employed the same method for a circular hatchway and pointed out its validity for studying the radiation of a baffled complex shaped structure, with no numerical integration needed for calculating the acoustic radiation but still required in the eigenanalysis of the structure's vibration.

A general approach for studying more than two sources is by means of the bridge theorem (Beranek and Mellow, 2019) or first product theorem (Williams, 1999), which states that it is possible to construct the directivity pattern of an array composed by N number of sources if the directivity of a single elementary source is known. Following this course, particular attention has been given to the study of transducer arrays, such as antennas in communications, line

[a]Electronic mail: carlos.garcia@utc.fr

arrays and directive speakers in audio, sonar in underwater acoustics, and ultrasonic transducers for medical purposes. In these cases, the study of mutual impedance plays a primordial role: Lee *et al.* (2004) studied the effect of the mutual impedance for optimizing the transducer placement in arrays present in sonars; Maadi *et al.* (2015) used the mutual radiation impedance for modelling capacitive micro-fabricated ultrasonic transducers (CMUTs). However, neither of these works included the phase component. Audoly (1991) used the Kirchhoff-Helmholtz integral to investigate the baffled and unbaffled cases for arrays, where the mutual impedance had to be solved numerically; Caronti *et al.* (2005) showed that an equivalent circuit (lumped method instead of radiators) does not always return accurate results due to the effect of the fluid load, but here the phase component plays an important role, allowing the energy to be focalized without changing the geometry of the array.

In this paper, we present a generalized method for constructing the radiation resistance and efficiency of distribution of circular pistons vibrating with arbitrary phases regardless of their size and position. The directivity pattern of the arrangement is calculated by means of the first product/bridge theorem and Bouwkamps's impedance theorem is then employed for deriving complete expressions of the radiation resistance and efficiency. The method described here is an extension of that presented by Beranek and Mellow (2019, pp. 699–713), which allowed us to explore the radiation of multiple sources. Some examples are presented when multiple sources of the same size are placed side by side. In these examples, the sources vibrate in-phase or in anti-phase. The radiation efficiency is then analyzed and compared to other kinds of structures such as a vibrating and oscillating sphere, circular radiators (Greenspan, 1979), or flat simply supported rectangular plates (Wallace, 1972), where the modal radiation patterns are found to be similar given the structure symmetry. With this approach, the underlying physics can be revealed allowing us to better understand the radiation traces, and the effects of the self- and mutual-efficiency.

II. RADIATION FROM PLANAR SOURCES

The pressure $\hat{p}$ of a baffled structure at any point in the space $\mathbf{r}$ is described by Rayleigh's integral,

$$\hat{p}(\mathbf{r}) = \frac{jk\rho_0 c}{2\pi}\int\int_S G(\mathbf{r}|\mathbf{r_0})\hat{v}(\mathbf{r_0})\mathrm{d}S, \tag{1}$$

in which k is the acoustic wavenumber and $\rho_0 c$ the specific impedance of a medium with volume density ρ_0 and speed of sound c. G is the Green function, $\hat{v}(\mathbf{r_0})$ the piston's surface velocity, and $\mathbf{r_0}$ the position vector on the surface S. The radiation impedance of a baffled structure Zs can be calculated directly using Bouwkamp's impedance theorem. Given a structure's directivity pattern for a vector $\mathbf{k}$, $D(\mathbf{k})$, the radiation impedance is calculated as

$$\begin{aligned} Zs &= Rs + iXs \\ &= \frac{k^2\rho_0 cS}{4\pi^2}\left(\int_0^{2\pi}\int_0^{\pi/2}|D(\mathbf{k})|^2\sin\theta\mathrm{d}\theta\mathrm{d}\phi \right. \\ &\quad \left. + \int_0^{2\pi}\int_{\pi/2+j0}^{\pi/2+j\infty}|D(\mathbf{k})|^2\sin\theta\mathrm{d}\theta\mathrm{d}\phi\right), \end{aligned} \tag{2}$$

where Rs and Xs are the specific radiation resistance and reactance, respectively. Since the reactive part does not radiate sound into the far-field, throughout the remainder of this paper only the resistive part will be considered.

III. RADIATION FROM MULTIPLE SOURCES

A. The first product and bridge theorems

The first product theorem for arrays was stated as follows (Williams, 1999, p. 49):

> "the directivity pattern of an array of N identical (size and shape) radiators is equal to the product of the directivity pattern of one of the radiators times the transform of the array of N baffled point sources positioned at the centers of the original radiators (now removed) with the same relative amplitude and phases as the original radiators."

The first product or bridge product theorem (illustrated in Fig. 1) addresses the multiplication of an elementary source's directivity by a point source in the Fourier space, where the relative distances to the sources appear now as in a phase component. Note that the phase component appears to be relative to multiple sources, so its placement is arbitrary.

Hence, by knowing the directivity of one baffled elementary source, the construction of a distribution of radiators becomes straightforward.

B. Single baffled piston

To obtain the directivity pattern of the baffled piston (illustrated in Fig. 2), a variety of approaches may be used. One road is to employ Eq. (1) with a uniform velocity field on the surface, use the image theory to calculate the Green function, and then integrate the result over a hemisphere, letting the distance tend to infinity. Other approaches may be followed; for example, by using Hankel and Bessel transforms of the pressure fields (Valier-Brasier, 2017), the

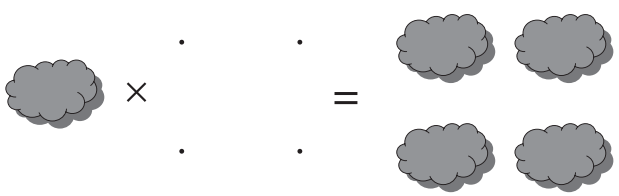

FIG. 1. The first product or bridge product theorem (illustration by Beranek and Mellow, 2019).

https://doi.org/10.1121/10.0013569

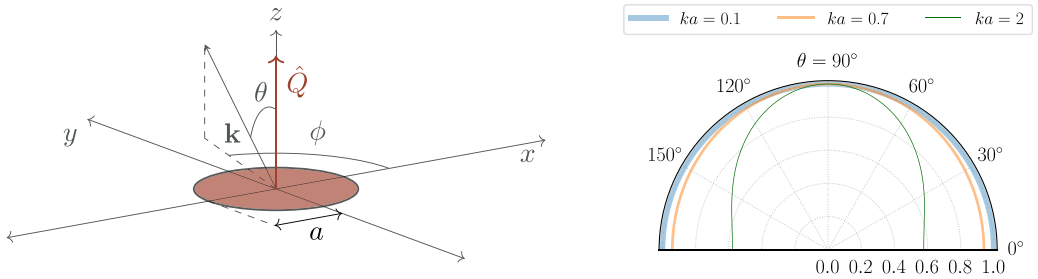

FIG. 2. (Color online) A piston of radius a in an infinite baffle with its directivity pattern for various values of ka. The amplitude $\hat{Q}$ is here and henceforth normalized to 1.

cylindrical Green's function in Eq. (1) or by taking the Fourier transform of the velocity field (Morse and Ingard, 1986, p. 377 and 381). All these approaches lead to

$$D(\theta,\phi) = \frac{2J_1(ka\sin\theta)}{ka\sin\theta}, \tag{3}$$

where J_n is the Bessel function of the first kind of n-order and θ and ϕ the azimuth and elevation angles, respectively. Inserting this into Eq. (2),

$$\begin{aligned} Rs &= \frac{(ka)^2\rho_0 c}{2\pi}\int_0^{2\pi}\int_0^{\pi/2}\frac{2J_1^2(ka\sin\theta)}{(ka)^2\sin\theta}\mathrm{d}\theta\mathrm{d}\phi, \\ &= \rho_0 c\left[1-\frac{J_1(2ka)}{ka}\right], \\ &= \rho_0 c\,\sigma_p(a) = R_p(a), \quad \text{the self-radiation resistance.} \end{aligned} \tag{4}$$

A detailed explanation of how to solve the previous integral can be found in King (1934, pp. 136–137). The radiation efficiency or self-radiation efficiency of the baffled piston σ_p is found by normalizing the radiation resistance by the acoustic characteristic impedance $\rho_0 c$. By expanding the Bessel function [see Eq. (33)], the self-radiation efficiency σ_p can be expressed in a series as

$$\sigma_p(a) = \frac{(ka)^2}{2} - \frac{(ka)^4}{2^2\cdot 3^1} + \frac{(ka)^6}{2^4\cdot 3^2}\cdots. \tag{5}$$

C. Two pistons with arbitrary phases

Two baffled pistons, as presented in Fig. 3, are vibrating with phases Φ_1 and Φ_2, respectively; $\Phi_i \in [0, 2\pi]$. The normalized by the surface directivity pattern is expressed as

$$\begin{aligned} D(\theta,\phi) = &\frac{a_1^2}{a_1^2+a_2^2}D_1(\theta)e^{i\Phi_1} \\ &+\frac{a_2^2}{a_1^2+a_2^2}D_2(\theta)e^{i(kd\sin\theta\cos\phi+\Phi_2)}, \end{aligned} \tag{6}$$

where D_1 and D_2 are defined by Eq. (3). The squared modulus of the directivity is

$$\begin{aligned} |D(\theta,\phi)|^2 = &\frac{2\pi^2}{(kS)^2}\left[\frac{2a_1^2J_1^2(ka_1\sin\theta)}{\sin^2\theta}+\frac{2a_2^2J_1^2(ka_2\sin\theta)}{\sin^2\theta}\right. \\ &+\frac{4a_1a_2J_1(ka_1\sin\theta)J_1(ka_2\sin\theta)}{\sin^2\theta} \\ &\left.\times\cos\left(kd\sin\theta\cos\phi+\Phi_{12}\right)\right], \end{aligned} \tag{7}$$

in which the total surface $S = \pi(a_1^2+a_2^2)$ and $\Phi_{12} = \Phi_1 - \Phi_2$. The specific radiation resistance Rs for the two pistons is expressed as

$$\begin{aligned} Rs = &\frac{\rho_0 c}{2S}\left[\int_0^{2\pi}\int_0^{\pi/2}\frac{2a_1^2J_1^2(ka_1\sin\theta)}{\sin\theta}\mathrm{d}\theta\mathrm{d}\phi\right. \\ &+\int_0^{2\pi}\int_0^{\pi/2}\frac{2a_2^2J_1^2(ka_2\sin\theta)}{\sin\theta}\mathrm{d}\theta\mathrm{d}\phi \\ &+2\int_0^{2\pi}\int_0^{\pi/2}\frac{2a_1a_2J_1(ka_1\sin\theta)J_1(ka_2\sin\theta)}{\sin\theta} \\ &\times\left(\cos\left(kd\sin\theta\cos\phi\right)\cos\Phi_{12}\right. \\ &\left.\left.+\sin\left(kd\sin\theta\cos\phi\right)\sin\Phi_{12}\right)\right]\mathrm{d}\theta\mathrm{d}\phi \\ = &\frac{\pi}{S}\left[a_1^2R_p(a_1)+a_2^2R_p(a_2)+2a_1a_2R_{2p}(a_1,a_2,d,\Phi_{12})\right]. \end{aligned} \tag{8}$$

$R_p(a_l)$ is the self-radiation resistance of piston l and R_{2p} is the mutual-radiation resistance between pistons 1 and 2. Employing the integral representation [refer to

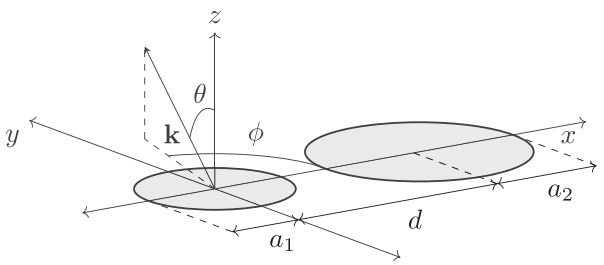

FIG. 3. Problem geometry: two pistons with radii a_1 and a_2, respectively, spaced a distance d and aligned on the x-axis.

Eqs. (27) and (28)] and setting $s = \sin\theta$, the mutual radiation is calculated as

$$\begin{aligned} R_{2p}(a_1, a_2, d, \Phi_{12}) &= 2\rho_0 c \int_0^{\pi/2} \frac{J_1(ka_1 \sin\theta) J_1(ka_2 \sin\theta)}{\sin\theta} \\ &\times (J_0(kd \sin\theta)\cos\Phi_{12} + \mathbf{H}_0(kd\sin\theta)\sin\Phi_{12})\mathrm{d}\theta, \\ &= 2\rho_0 c \int_0^1 \frac{J_1(ka_1 s) J_1(ka_2 s)}{s\sqrt{1-s^2}} \\ &\times (J_0(kds)\cos\Phi_{12} + \mathbf{H}_0(kds)\sin\Phi_{12})\mathrm{d}s; \end{aligned} \tag{9}$$

Lommel's expansion [see Eq. (30)] is used to expand J_1, then Bessel and Struve functions [Eqs. (31) and (32)] are integrated to find

$$\begin{aligned} R_{2p}(a_1, a_2, d, \Phi_{12}) &= 2\rho_0 c \sum_{m=0}^{\infty}\sum_{n=0}^{\infty} \left(\frac{ka_1}{2}\right)^m \left(\frac{ka_2}{2}\right)^n \frac{J_{m+1}(ka_1) J_{n+1}(ka_2)}{m!n!} \\ &\times \int_0^1 [J_0(kds)\cos\Phi_{12} + \mathbf{H}_0(kds)\sin\Phi_{12}] \\ &\times (1-s^2)^{m+n-1/2} s\mathrm{d}s, \\ &= \rho_0 c \frac{2}{\sqrt{\pi}} \sum_{m=0}^{\infty}\sum_{n=0}^{\infty} \left(\frac{a_1}{d}\right)^m \left(\frac{a_2}{d}\right)^n \\ &\times \frac{J_{m+1}(ka_1) J_{n+1}(ka_2)}{m!n!} \Gamma\left(m+n+\frac{1}{2}\right) \\ &\times [j_{m+n}(kd)\cos\Phi_{12} + \mathbf{h}_{m+n}(kd)\sin\Phi_{12}]. \end{aligned} \tag{10}$$

The gamma function of a positive half-integer is defined for any $n \in \mathbb{Z}^+$ as $\Gamma[n + (1/2)] = \sqrt{\pi}/2^n(2n-1)!$ and j_m and $\mathbf{h}_m$ are the spherical Bessel and Struve functions of the first kind of order m, respectively [refer to Eqs. (34) and (35)] This approach to calculating the mutual radiation impedance Z_{12} for pistons in phase, was taken first by Pritchard (1960), demonstrating an absolute convergence of the series when $a_1 a_2 < d^2$. In the same lane, Chan (1967) and Beranek and Mellow (2019, pp. 699–713) studied the case for two pistons in phase with arbitrary dimensions. In all these cases, by placing the pistons along the y axis instead of the x-axis, the previous derivation of the expressions becomes clearer, as the classical Bessel integral representation appears [Eq. (29) instead of Eq. (27)]. When the pistons are in phase or in anti-phase, the mutual-radiation reactance can be calculated following the same procedure; however, for an arbitrary phase, no simple expression can be obtained.

The mutual-radiation efficiency is calculated by dividing the mutual-radiation resistance by the free-space resistance $\rho_0 c$,

$$\sigma_{2p} = R_{2p}/\rho_0 c. \tag{11}$$

For two pistons with the same radii $a_1 = a_2 = a$, it is possible to take the first three terms in Eq. (10) and the trigonometric representation of the spherical Bessel function to find

$$\begin{aligned} \sigma_{2p}(a, d) \simeq 2(J_1^2(ka) &+ \frac{a}{d}\Upsilon J_1(ka) J_2(ka) \\ &+ \left(\frac{a}{d}\right)^2 \Lambda J_2^2(ka)) \frac{\sin kd}{kd}, \end{aligned} \tag{12}$$

where $\Upsilon = 1/kd - \cot(kd)$, $\Lambda = (3/4)[(3\Upsilon/kd) - 1]$ and which represents a good approximation for the mutual radiation efficiency when $d \geq 2a$, as observed in Fig. 4. Moreover, taking only the zero-order terms in $a_{1,2}/d$, it is for $m, n = 0$ and if $a_1 a_2 \ll d^2$ it is possible to derive the coefficients of the Acoustic Radiation Resistance Matrix (ARM) described by Hashimoto [2001, Eq. (2)], here normalized by the specific impedance,

$$\sigma_{2p}(a_1, a_2, d) \simeq 2J_1(ka_1) J_1(ka_2) \frac{\sin kd}{kd}. \tag{13}$$

In addition, if the no-overlapping condition $d \geq a_1 + a_2$ is fulfilled, the first zero is given by the sinus function in Eq. (13), that is when $kd = \pi$, and if $d = 2a$, then it occurs when $ka = \pi/2$ as depicted in Fig. 4. The influence of the mutual efficiency is illustrated in Fig. 5 as a function of the distance between the pistons and the phase.

Finally, the complete formulation of σ for two pistons becomes

$$\begin{aligned} \sigma(a_1, a_2, d, \Phi_{12}) = \frac{\pi}{S}\big[a_1^2 \sigma_p(a_1) &+ a_2^2 \sigma_p(a_2) \\ &+ 2a_1 a_2 \sigma_{2p}(a_1, a_2, d, \Phi_{12})\big]. \end{aligned} \tag{14}$$

Keeping in mind that the phase term Φ_{12} equals zero or π when the pistons vibrate in phase or in anti-phase, the Struve function in Eq. (10) cancels and the mutual radiation efficiency becomes

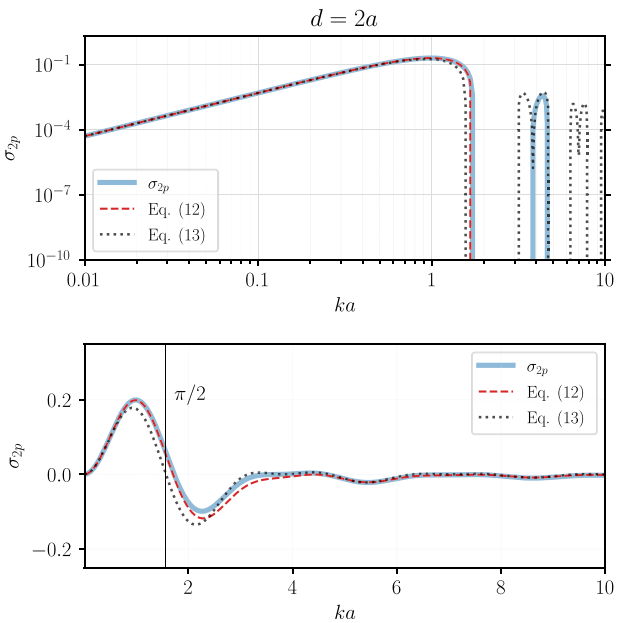

FIG. 4. (Color online) Mutual-radiation efficiency of two pistons of the same size at the minimum distance without overlapping, $d = 2a$. The first zero arrives near $ka = \pi/2$.

https://doi.org/10.1121/10.0013569

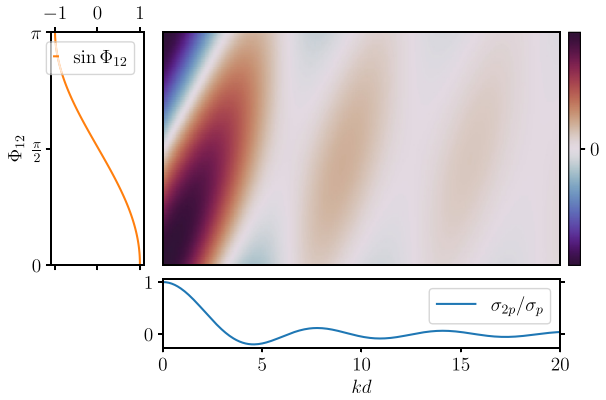

FIG. 5. (Color online) Ratio σ_{2p}/σ_p for $ka = 1$ as a function of kd and the relative phase between two pistons Φ_{12} of equal area.

$$\sigma_{2p}(a_1, a_2, d, \Phi_{12} + \pi) = -\sigma_{2p}(a_1, a_2, d, \Phi_{12}). \tag{15}$$

By expanding the first terms of σ_{2p} when $a_1 = a_2 = a$ and $d = 2a$,

$$\sigma_{2p}(a, d = 2a) = \frac{(ka)^2}{2} - \frac{11(ka)^4}{2^2 \cdot 3!} + \frac{233(ka)^6}{2^4 \cdot 5!} - \cdots \tag{16}$$

Note that the first term is the same as in the piston case [see Eq. (5)], and the limit when $ka \gg 1 \to 0$. In a general sense, a monopolar behaviour will appear if the term proportional to $(ka)^2$ persists. If this term is cancelled and the term proportional to $(ka)^4$ remains, the pistons radiate as a dipole. By eliminating both terms, a quadrupole radiation will be observed. In Secs. III D, III E, and V, these cases will be discussed in more detail.

D. Two pistons vibrating in phase

When the pistons vibrate in phase, as in Fig. 6, $\Phi_{12} = 0$. This cancels the sinus and leaves unchanged the R_{2p} function in Eq. (10). Finally, the radiation efficiency can be written as

$$\sigma_{monopole}{}^{\oplus}_{\oplus} = \sigma_{monopole}{}^{\ominus}_{\ominus} = \sigma_p(a) + \sigma_{2p}(a, d), \quad \text{if} \quad a_1 = a_2 = a. \tag{17}$$

The low-frequency limits for both components are the same, and the radiation efficiency of the two pistons vibrating in phase is similar to a piston whose surface is doubled.

E. Two pistons vibrating in anti-phase

The directivity pattern of two pistons vibrating in anti-phase makes $\Phi_{12} = \pm\pi$ (Fig. 7). This changes the sign of the mutual radiation efficiency σ_{2p} in Eq. (14) from a + into a –, and also eliminates the sinus coefficient in Eq. (10), as in the previous case. Note that the first term proportional to $(ka)^2$ is cancelled between the self- and mutual parts, which produces a dipolar radiation pattern. For pistons with equal radii

$$\sigma_{dipole}{}^{\oplus}_{\ominus} = \sigma_p(a) - \sigma_{2p}(a, d), \quad \text{if} \quad a_1 = a_2 = a. \tag{18}$$

In Fig. 8, the characteristic monopolar radiation slope of 6 dB/octave can be clearly identified. This slope is the same for one single radiator as it is for two radiators in phase. Also, this slope describes the radiation of monopole point sources, pulsating spheres [Valier-Brasier, 2017, Eq. (3.38)], and the spherical harmonics of degree zero [Wu *et al.*, 2014, Eq. (19)], as well as circular simply supported or clamped radiators [Greenspan, 1979, Eqs. (45b), (47b)] and [Aarts and Janssen, 2009, Eq. (36)].

As seen in Eq. (5), the monopolar behaviour is proportional to $(ka)^2$, while in the dipole case, this term counteracts, leaving the characteristic dipolar-slope proportional to $(ka)^4$ at low frequencies. Consequently, the radiation efficiency increases by 12 dB/octave, similar to oscillating spheres [Valier-Brasier, 2017, Eq. (3.39)] and first-degree spherical harmonics.

F. Three pistons on the plane

Three radiators, whose radii are a_1, a_2, and a_3, respectively, are placed on the plane xy. The vector $\mathbf{r}_i$ describes the position from the origin to the i source's center, as depicted in Fig. 9. The directivity pattern using the bridge product theorem takes the general form

$$D(\mathbf{k}) = \frac{\pi}{S} \sum_{l=1}^{N} a_l^2 D_l(\mathbf{k}) e^{i(\mathbf{k}\cdot\mathbf{r}_l + \Phi_l)}, \tag{19}$$

where $N = 3$ in this case. The squared modulus of the directivity is expressed as

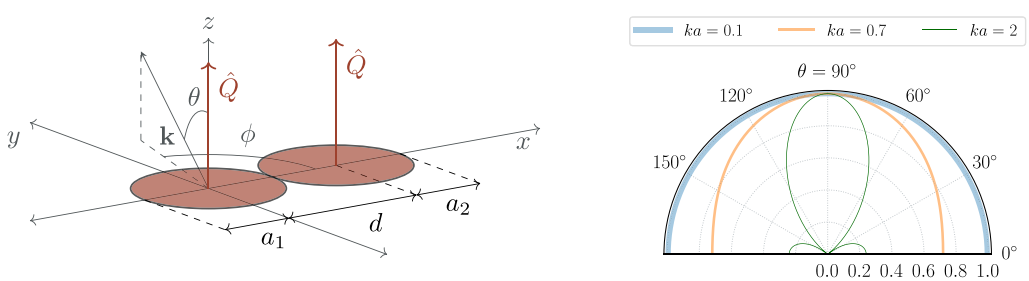

FIG. 6. (Color online) (a) Pistons vibrating in phase having the same radius $a_1 = a_2 = a$ at a distance $d = 2a$. b) The directivity pattern of the array for $\phi = 0$.

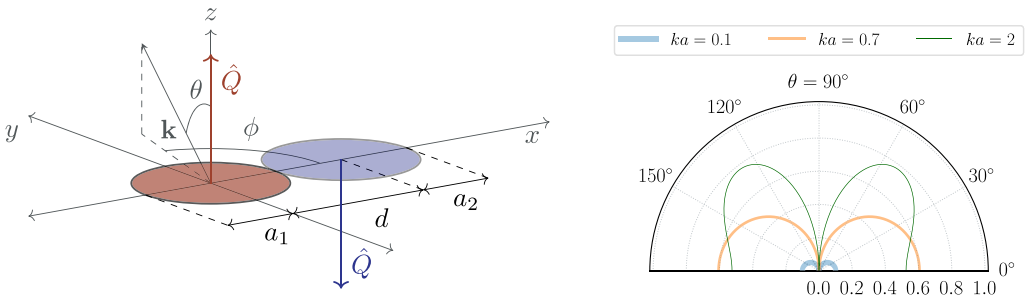

FIG. 7. (Color online) (a) Pistons vibrating in anti-phase at a distance $d = 2a$ with the same radius $a_1 = a_2 = a$. Positive amplitudes are displayed in red and negative amplitudes in blue. (b) The directivity pattern of the array ($\Phi_{12} = \pi$).

$$
\begin{aligned}
|D(\mathbf{k})|^2 = \frac{\pi^2}{S^2}\Bigg[&\sum_{l=1}^{3} a_l^4 D_l^2(\mathbf{k}) + a_1^2 a_2^2 D_1(\mathbf{k}) D_2(\mathbf{k}) \\
&\times \left(e^{i[\mathbf{k}\cdot(\mathbf{r}_1-\mathbf{r}_2)+\Phi_1-\Phi_2]} + e^{-i[\mathbf{k}\cdot(\mathbf{r}_1-\mathbf{r}_2)+\Phi_1-\Phi_2]}\right) \\
&+ a_2^2 a_3^2 D_2(\mathbf{k}) D_3(\mathbf{k}) \\
&\times \left(e^{i[\mathbf{k}\cdot(\mathbf{r}_2-\mathbf{r}_3)+\Phi_2-\Phi_3]} + e^{-i[\mathbf{k}\cdot(\mathbf{r}_2-\mathbf{r}_3)+\Phi_2-\Phi_3]}\right) \\
&+ a_3^2 a_1^2 D_3(\mathbf{k}) D_1(\mathbf{k}) \\
&\times \left(e^{i[\mathbf{k}\cdot(\mathbf{r}_3-\mathbf{r}_1)+\Phi_3-\Phi_1]} + e^{-i[\mathbf{k}\cdot(\mathbf{r}_3-\mathbf{r}_1)+\Phi_3-\Phi_1]}\right)\Bigg] \\
= \frac{\pi^2}{S^2}\Bigg[&\sum_{l=1}^{3} a_l^4 D_l^2(\mathbf{k}) + 2a_1^2 a_2^2 D_1(\mathbf{k}) D_2(\mathbf{k}) \\
&\times \cos\left(\mathbf{k}\cdot(\mathbf{r}_1-\mathbf{r}_2)+\Phi_{12}\right) \\
&+ 2a_2^2 a_3^2 D_2(\mathbf{k}) D_3(\mathbf{k}) \cos\left(\mathbf{k}\cdot(\mathbf{r}_2-\mathbf{r}_3)+\Phi_{23}\right) \\
&+ 2a_3^2 a_1^2 D_3(\mathbf{k}) D_1(\mathbf{k}) \cos\left(\mathbf{k}\cdot(\mathbf{r}_3-\mathbf{r}_1)+\Phi_{31}\right)\Bigg].
\end{aligned}
\tag{20}
$$

In the new coordinate axis, it is possible to see the contribution of each piston and the cross terms, which, after integration, will result in the self- and mutual-radiation between each pair of pistons. Due to the circular symmetry of the pistons, D_l does not depend on ϕ but only varies with θ, which is unchanged in the new coordinate system, as depicted in Fig. 9. Hence, it is possible to reallocate the system of coordinates as convenience to calculate the radiation resistance. Consider, for example, the mutual radiation resistance between pistons 1 and 3,

$$
\begin{aligned}
&R_{2p}(a_1, a_3, \mathbf{k}\cdot(\mathbf{r}_3-\mathbf{r}_1), \Phi_{13}) \\
&\quad = \frac{2k\rho_0 c}{S}\int_0^{2\pi}\int_0^{\pi/2} a_1^2 a_3^2 D_1(\mathbf{k}) D_3(\mathbf{k}) \\
&\qquad \times \cos\left(\mathbf{k}\cdot(\mathbf{r}_3-\mathbf{r}_1)+\Phi_{31}\right)\sin\theta \mathrm{d}\theta\mathrm{d}\phi \\
&\quad = \frac{2k\rho_0 c}{S}\int_0^{2\pi}\int_0^{\pi/2} a_1^2 a_3^2 D_1(\theta',\phi') D_3(\theta',\phi') \\
&\qquad \times \cos\left(kd_{31}\sin\theta'\cos\phi'+\Phi_{13}\right)\sin\theta' \mathrm{d}\theta'\mathrm{d}\phi' \\
&\quad = R_{2p}(a_1, a_3, d_{13}, \Phi_{13}).
\end{aligned}
\tag{21}
$$

Clearly, we are able to take advantage of the local coordinates due to the symmetry of the circular piston, thereby compacting the problem and leaving only two functions to define the radiation: the self- and mutual-radiation resistance and efficiency.

IV. RADIATION RESISTANCE AND EFFICIENCY OF A RANDOM DISTRIBUTION OF PISTONS

It is now possible to express the radiation of a distribution of N baffled sources, regardless of their radius, position, or phase.

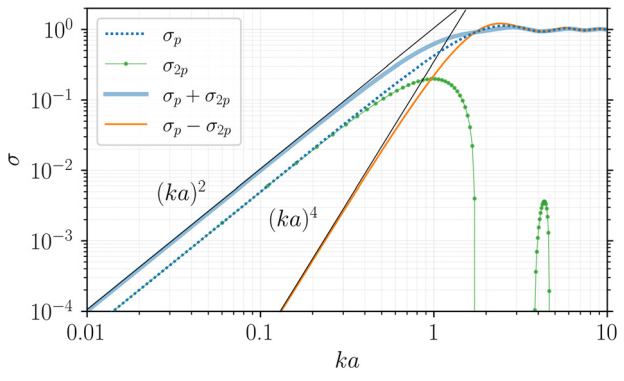

FIG. 8. (Color online) Radiation efficiency, from top to bottom: one single piston (dotted blue), mutual radiation efficiency of two pistons (dotted green), pistons vibrating in phase (solid blue), pistons vibrating in anti-phase (solid orange). All pistons have the same radius a and are separated the same distance $d = 2a$.

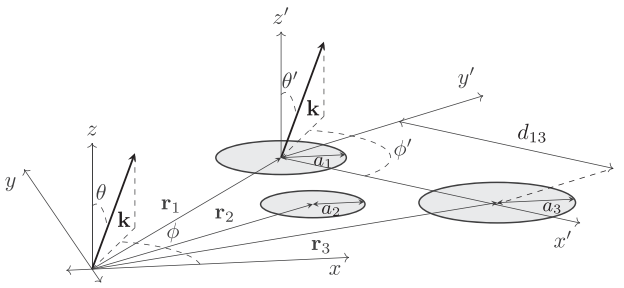

FIG. 9. Three pistons placed on the plane xy. The bridge product theorem can be implemented more straightforwardly by changing the axis origin to coincide with the piston's center and utilizing directly the distances between each pair of pistons.

https://doi.org/10.1121/10.0013569

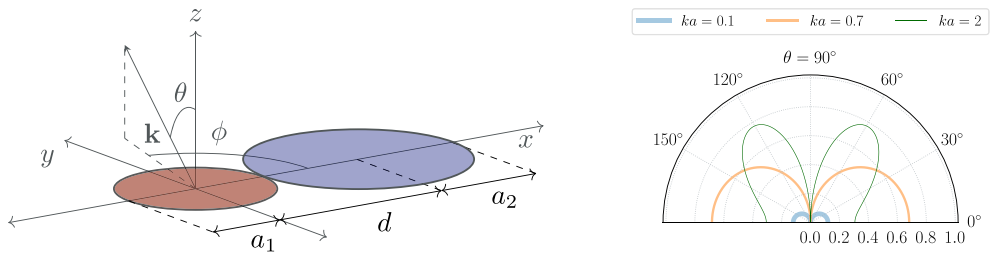

a) b)

FIG. 10. (Color online) (a) Vibrating pistons with different areas vibrating in anti-phase. (b) Directivity of the dipole when $\phi = 0$.

The radiation parameters Rs and σ of the arrangement can be expressed as a linear combination of the contribution of every single piston plus a term coming from the mutual radiation of each pair of radiators. The mutual radiation term is a function of each piston radius a_i, the distance between each pair of sources $d_{ij} = \|\mathbf{r}_i - \mathbf{r}_j\|$, and the vibrating phase Φ_i of each radiator. Therefore, the radiation efficiency can be summarized as

$$\sigma = \frac{\pi}{S}\left(\sum_{l=1}^{N} a_l^2 \sigma_p(a_l) + 2\sum_{i=1}^{N}\sum_{j>i}^{N} a_i a_j \sigma_{2p}(a_i, a_j, d_{ij}, \Phi_{ij})\right). \quad (22)$$

Note than only two types of functions are presented in the previous equation: σ_p, defined in Eq. (4), and σ_{2p}, developed from Eqs. (8)–(11). Section III C provides useful and fast approximations of mutual-radiation efficiency [see Eqs. (12) and (13)], even though the double series in the complete expression of σ_{2p} converges fast.

V. ANALYSIS OF THE RADIATION EFFICIENCY IN SOME TYPICAL CASES

A. Dipole with non-zero flux

Taking two pistons vibrating in anti-phase with areas $S_2 = 2S_1$, as seen in Fig. 10, we find

$$\sigma_d = \frac{\pi}{S}\left[a_1^2 \sigma_p(a_1) + a_2^2 \sigma_p(a_2) - 2a_1 a_2 \sigma_{2p}(a_1, a_2, d)\right]. \quad (23)$$

As shown in Fig. 11, annulling the low-frequency dipole slope is the main effect when two pistons are of different sizes. For small values of ka, the term $\sim(ka)^2$ does not cancel itself out, resulting in a small monopole. This monopole radiates more energy in the low-frequency range than a single piston, whose surface would be $S = S_2 - S_1$.

B. Three sources aligned and in "L" shape

In this case, two dipoles are formed, sharing one single radiator in anti-phase. The dipoles are spaced a distance $d = 2a$ in both cases and have the same radius a, as illustrated in Fig. 13.

The first case leaves the pistons vibrating in phase separated a distance $d_{23} = 2d$ and for the second case $d_{23} = \sqrt{2}d$. The distance $d_{12} = d_{13} = d$ in both examples, which results in

$$\sigma_t = \sigma_p(a) - \frac{4}{3}\sigma_{2p}(a, d) + \frac{2}{3}\sigma_{2p}(a, d_{23}),$$
$$d_{23} = \begin{cases} 2d & \text{if aligned,} \\ \sqrt{2}d, & \text{if in "L."} \end{cases} \quad (24)$$

When the radiators are aligned, as exposed in Fig. 12(a), two different regions are well identifiable: the monopolar behaviour in the low-frequency regime when $ka \ll 1$ comes from the contribution of all pistons plus the contribution of the

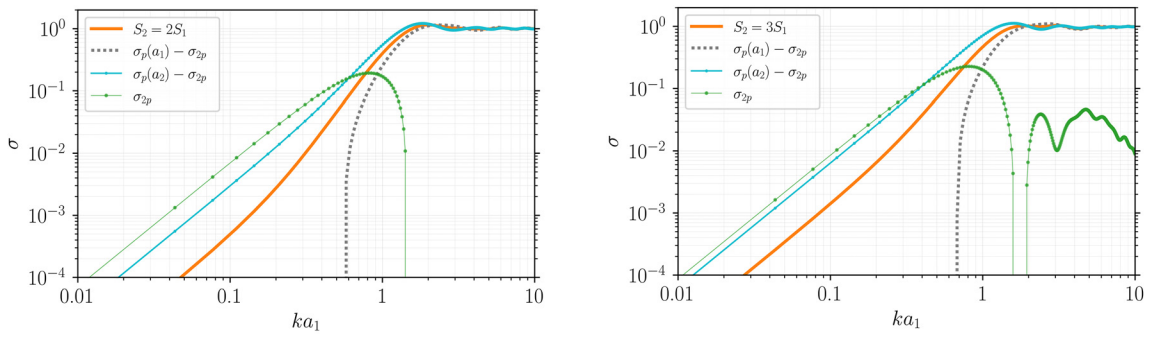

a) b)

FIG. 11. (Color online) Dipole when one of the piston's area is (a) twice that of the other, (b) triple that of the other.

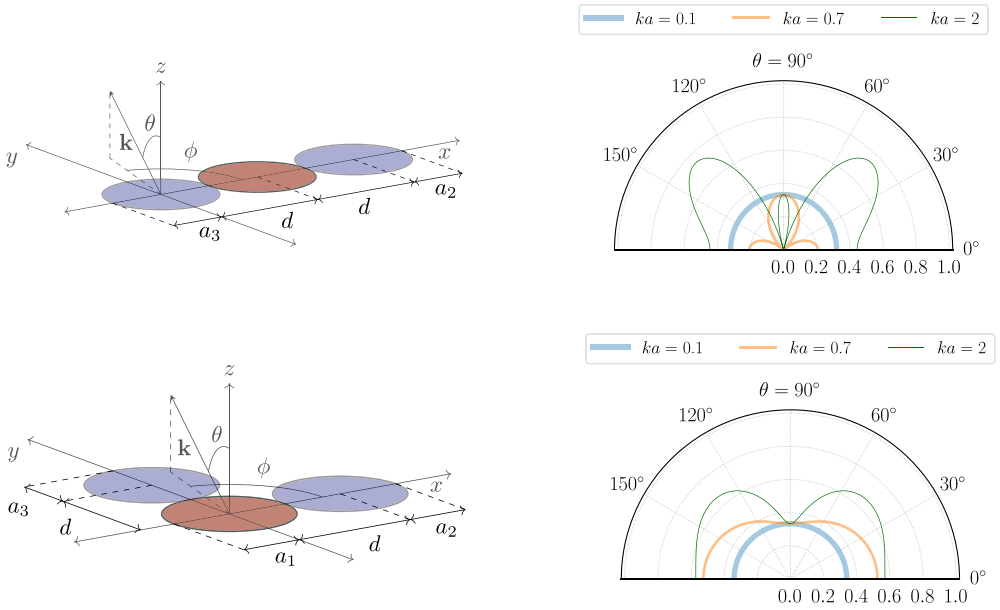

FIG. 12. (Color online) Three piston with the same radius $a_1 = a_2 = a_3 = a$ and $d = 2a$. The distance between the pistons in phase (in blue) is smaller in the second case. The directivity is plotted on the axis of symmetry: $\phi = 0$ in the first case and $\phi = \pi/4$ when the pistons are aligned in "L". A three-dimensional (3D) plot is provided in the supplemental material (García *et al.*, 2022).

pistons vibrating in phase at $\sqrt{2}d$. When $1 \leq ka < 2$, the dipole regime with its characteristic slope appears at first sight and can also be identified in the directivity pattern in Fig. 12. These two tendencies in the radiation efficiency are also present in the mode (1,3) in a simply supported rectangular plate (Wallace, 1972). In the second case [Fig. 13(b)], the monopole dominates the low frequency regime even when ka approaches the unity. The separation between monopolar and dipolar radiation cannot be identified and the dipole effect is seen to be suppressed, clearly appreciated in the efficiency plot and the directivity pattern in Fig. 12. As shown in Fig. 13(b), this effect is solely the result of the pistons vibrating in phase at different distances, whose mutual radiating efficiency is illustrated in green dotted lines. The orange dashed lines represent the contribution of each pair of pistons separated a distance d, and the overlapping between these two traces marks the transition between monopolar and dipolar radiation. In addition, the evolution of the slope is similar to that of the dipole case exposed in Sec. III E.

C. Quadrupole

Four sources are arranged along one axis in one case, and in a squared array in the other, as shown in Fig. 14. In terms of radiation efficiency,

$$\sigma_q = \sigma_p(a) - \frac{3}{2}\sigma_{2p}(a,d) + \sigma_{2p}(a,2d) - \frac{1}{2}\sigma_{2p}(a,3d), \quad (25)$$

if the pistons are aligned, and

$$\sigma_q = \sigma_p(a) - 2\sigma_{2p}(a,d) + \sigma_{2p}\left(a,\sqrt{2}d\right), \quad (26)$$

if they are placed in a squared arrangement. It can be seen in Fig. 15(a) that only half of the amplitude of the two most distant pistons is not cancelled, so the remainder radiator becomes a dipole and then the slope changes into a quadrupole (18 dB/octave). The distance between each pair is $2d$ and the transition between regimes is around $ka = 1$. The dipole and quadrupole behaviour can also be seen in the

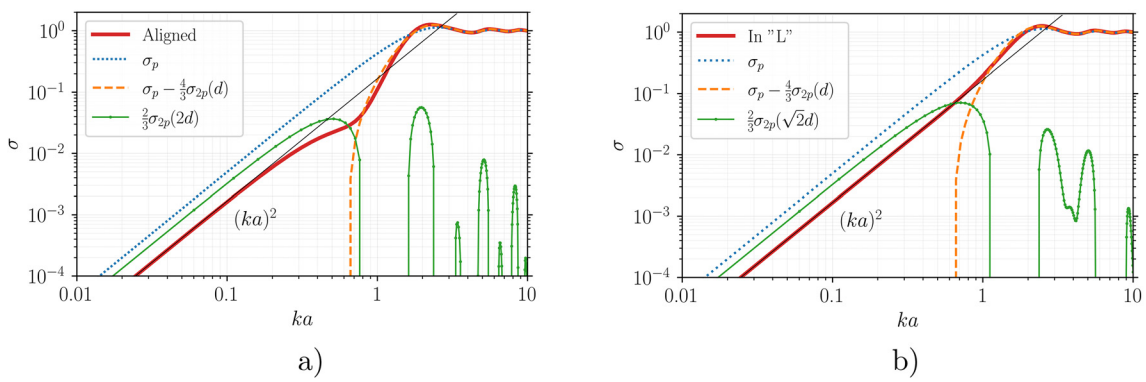

FIG. 13. (Color online) Three pistons, two of them are separated of (a) $d_{23} = 2d$ and (b) $d_{23} = \sqrt{2}d$.

https://doi.org/10.1121/10.0013569

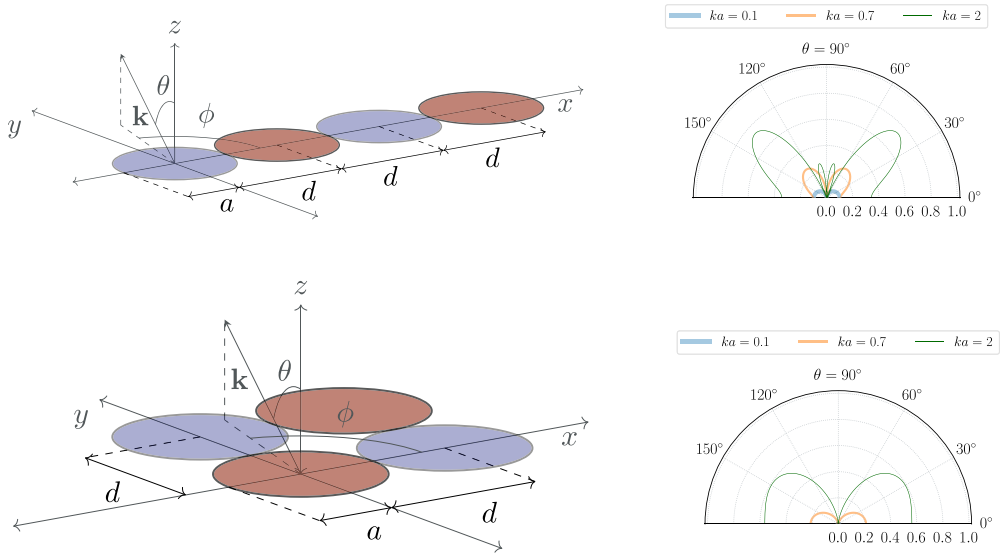

FIG. 14. (Color online) Four pistons (a) arranged in a line and in a square with two of the vibrating with positive phase and the other in anti-phase. (b) Directivity of each array for $\phi = 0$ when the pistons are disposed on the axis x, and $\phi = \pi/4$ or $\phi = 3\pi/4$ when the pistons are disposed in a square array. See the supplemental material (García *et al.*, 2022) for some 3D plots.

directivity pattern in Fig. 14. When the pistons form a square, due to the symmetry between the sources, the dipole effect is fully cancelled, leaving the structure radiating as a quadrupole [see Fig. 15(b)], with a slope proportional to $(ka)^6$ as also seen in the spherical harmonics of degree 2 [Wu *et al.*, 2014, Eq. (19)] Both cases are also well identifiable in the simply supported plate presented by Wallace (1972).

VI. CONCLUSION

In this paper, we present a method for calculating the far-field radiation of distribution of pistons with different sizes, placed arbitrarily on a baffled plane and vibrating with arbitrary phases. This approach allows for the direct calculation of radiation resistance and efficiency of any type of piston arrangement, which extends the work of Pritchard (1960) and Beranek and Mellow (2019). The core of this analytical formulation lies in the calculation of only the self- and mutual-radiation components including a phase component. The circular piston's symmetry enables the derivation of analytical formulas for any arrangement without the need for numerical integration. The acoustic radiation of this type of structure can be analyzed by the contribution of each term, resulting in simple expressions formed by the self- and mutual-radiation of the sources, the phase, and the distance. By using this approach, we can gain some insight into the tendencies and physical understanding of radiation efficiency. This method can be developed further to take into account axisymmetric non-uniform velocity profiles, as in resilient radiators, or to include the near field effects induced by the reactance, which are not considered in this paper, but that may occur when two sources are too close to each other, or when the fluid loading cannot be ignored and may couple the vibration of several sources at once. The versatility of this approach allows different scenarios to be explored, such as the radiation present in ultrasonic instrumentation; the inverse problem presented in antennas. In classic flat vibro-acoustic structures, as plates or membranes, the mode shapes could be approached by a combination of vibrating pistons to a certain extent. The method that we have developed here can be used to predict the modal radiation efficiency of this kind of structure, revealing the underlying physics, where numerical solutions have to be implemented in the absence of more intuitive approaches.

VII. INTEGRALS

Lommel integral representation [Watson, 1966, Eq. (1), p. 47],

$$J_\nu(z) = \frac{1}{\Gamma\left(\nu+\frac{1}{2}\right)\Gamma\left(\frac{1}{2}\right)}\left(\frac{z}{2}\right)^\nu \times \int_0^\pi \sin^{2\nu}(\phi)\cos(z\cos\phi)\mathrm{d}\phi, \quad \left[\mathrm{Re}\,\nu > -\frac{1}{2}\right]. \tag{27}$$

Integral representation of the Struve function [Zwillinger *et al.*, 2014, Eq. (3.715), p. 16],

$$\int_0^{\pi/2} \sin(z\cos\phi)\sin^{2\nu}\phi\mathrm{d}\phi = \frac{\sqrt{\pi}}{2}\left(\frac{2}{z}\right)^\nu \Gamma\left(\nu+\frac{1}{2}\right)\mathbf{H}_\nu(z), \quad \left[\mathrm{Re}\,\nu > -\frac{1}{2}\right]. \tag{28}$$

Integral representation of the Bessel function [Watson, 1966, Eq. (1), p. 19],

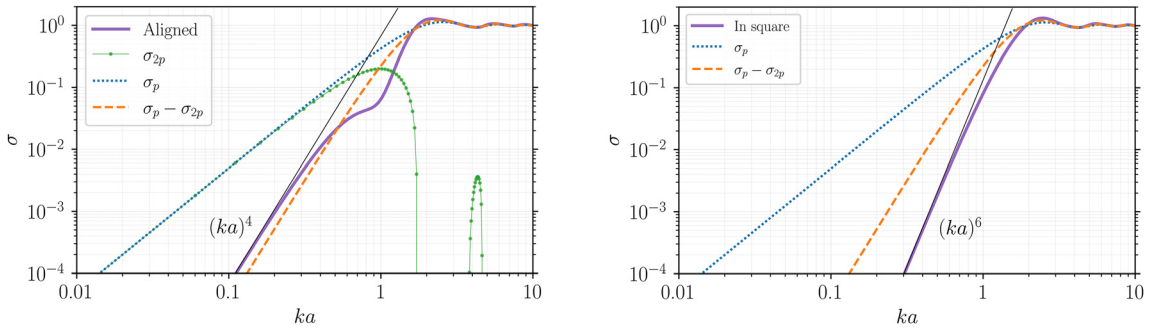

FIG. 15. (Color online) Four pistons (a) aligned on the x axis at a constant distance $d = 2a$, (b) forming a square. The distance between the pistons in phase is $\sqrt{2}d$.

$$J_n(z) = \frac{1}{2\pi}\int_0^{2\pi} \cos\left(z\sin\phi - n\phi\right)\mathrm{d}\phi. \tag{29}$$

Lommel expansion [Beranek and Mellow, 2019, Eq. (13.343)],

$$J_\nu(bz) = z^\nu \sum_{n=0}^{\infty} \left(\frac{b}{2}\right)^n \frac{(1-z^2)^n}{n!} J_{\nu+n}(b). \tag{30}$$

Sonine's integral [Beranek and Mellow, 2019, Eq. (A2.96)],

$$\int_0^a \left(1-\frac{z^2}{a^2}\right)^{\mu+\frac{1}{2}} J_0(bz) z\mathrm{d}z = \frac{a^2}{2}\Gamma\left(\mu+\frac{3}{2}\right) \times \left(\frac{2}{ab}\right)^{\mu+\frac{3}{2}} J_{\mu+\frac{3}{2}}(ab). \tag{31}$$

Integral of the Struve function [Zwillinger *et al.*, 2014, Eq. (6.815), p. 1],

$$\int_0^1 z^{\frac{1}{2}\nu}(1-z)^{\mu-1}\mathbf{H}_\nu\left(b\sqrt{z}\right)\mathrm{d}z = 2^\mu b^{-\mu}\Gamma(\mu)\mathbf{H}_{\mu+\nu}(b), \quad \left[\mathrm{Re}\,\nu > -\frac{3}{2},\ \mathrm{Re}\,\mu > 0\right]. \tag{32}$$

Bessel expansion,

$$J_n(z) \quad = \sum_{k=0}^{\infty} \frac{(-1)^k}{k!\Gamma(n+k+1)}\left(\frac{z}{2}\right)^{n+2k}. \tag{33}$$

Bessel trigonometric half-integer expansion,

$$J_{n+\frac{1}{2}}(z) = (-1)^n z^{n+\frac{1}{2}}\sqrt{\frac{2}{\pi}}\frac{d^n}{(zdz)^n}\left(\frac{\sin z}{z}\right). \tag{34}$$

Spherical Bessel function (Rayleigh formula),

$$j_n(z) = (-z)^n\left(\frac{1}{z}\frac{d}{dz}\right)^n \frac{\sin z}{z}. \tag{35}$$

Aarts, R. M., and Janssen, A. J. E. M. (**2009**). "Sound radiation quantities arising from a resilient circular radiator," J. Acoust. Soc. Am. **126**(4), 1776–1787.

Arenas, J. P. (**2008**). "Numerical computation of the sound radiation from a planar baffled vibrating surface," J. Comput. Acoust. **16**(3), 321–341.

Arenas, J. P. (**2009**). "On the sound radiation from a circular hatchway," Int. J. Occupational Safety Ergonom. **15**(4), 401–407.

Audoly, C. (**1991**). "Some aspects of acoustic interactions in sonar transducer arrays," J. Acoust. Soc. Am. **89**(3), 1428–1433.

Babinet, J. (**1837**). "Mémoires d'optique météorologique" ("Optical meteorology memoirs"), C. R. Acad Sci **78**(6), 638–648.

Beranek, L. L., and Mellow, T. J. (**2019**). *Acoustics Sound Fields, Transducers and Vibration*, second edition ed. (Academic Press, New York).

Bouwkamp, C. (**1970**). "Theoretical and numerical treatment of diffraction through a circular aperture," IEEE Trans. Antennas Propagat. **18**(2), 152–176.

Bouwkamp, C. J. (**1945**). "A contribution to the theory of acoustic radiation," Philips Res. Rep. **1**, 251–277.

Caronti, A., Savoia, A., Caliano, G., and Pappalardo, M. (**2005**). "Acoustic coupling in capacitive microfabricated ultrasonic transducers: Modeling and experiments," IEEE Trans. Ultrason, Ferroelect, Freq. Contr. **52**(12), 2220–2234.

Chan, K. (**1967**). "Mutual acoustic impedance between flexible disks of different sizes in an infinite rigid plane," J. Acoust. Soc. Am. **42**(5), 1060–1063.

Crane, P. H. G. (**1967**). "Method for the calculation of the acoustic radiation impedance of unbaffled and partially baffled piston sources," J. Sound Vib. **5**(2), 257–277.

Elliott, S. J., and Johnson, M. E. (**1993**). "Radiation modes and the active control of sound power," J. Acoust. Soc. Am. **94**(4), 2194–2204.

García A., C., Dauchez, N., and Lefebvre, G. (**2022**). "Supplemental material: Directivity of sources.," https://nbviewer.org/github/charlie-garcia/radiation_piston/blob/main/directivity_plots.ipynb. (Last viewed August 13, 2022).

Greenspan, M. (**1979**). "Piston radiator: Some extensions of the theory," J. Acoust. Soc. Am. **65**(3), 608–621.

Hashimoto, N. (**2001**). "Measurement of sound radiation efficiency by the discrete calculation method," Appl. Acoust. **62**(4), 429–446.

King, L. V. (**1934**). " on the acoustic radiation field of the piezo-electric oscillator and the effect of viscosity on transmission," Can. J. Res. **11**, 135–155.

Lee, H., Tak, J., Moon, W., and Lim, G. (**2004**). "Effects of mutual impedance on the radiation characteristics of transducer arrays," J. Acoust. Soc. Am. **115**(2), 666–679.

Maadi, M., Chee, R., and Zemp, R. J. (**2015**). "Mutual radiation impedance for modeling of multi-frequency CMUT arrays," in *Proceedings of the 2015 IEEE International Ultrasonics Symposium (IUS)*, October 21–24, Taipei, Taiwan, pp. 1–4.

Mellow, T., and Kärkkäinen, L. (**2016**). "Expansions for the radiation impedance of a rectangular piston in an infinite baffle," J. Acoust. Soc. Am. **140**(4), 2867–2875.

Morse, P. M., and Ingard, K. U. (**1986**). *Theoretical Acoustics* (Princeton University Press, Princeton, NJ).

Naghshineh, K., and Koopmann, G. H. (**1991**). "A design method for achieving weak radiator structures using active vibration control," J. Acoust. Soc. Am. **90**(4), 2270–2270.

Porter, D. T. (**1964**). " 'Self' and mutual-radiation impedance and beam patterns for flexural disks in a rigid plane," J. Acoust. Soc. Am. **36**(6), 1154–1161.

Pritchard, R. L. (**1960**). "Mutual acoustic impedance between radiators in an infinite rigid plane," J. Acoust. Soc. Am. **32**(6), 730–737.

Rayleigh, L. (**1897**). "On the passage of waves through apertures in Plane screens, and allied problems," Philos. Mag. **43**(263), 259–272.
Rayleigh, L. (**1945**). *The Theory of Sound*, 2nd ed. (Dover Publications, New York).
Stepanishen, P. R. (**1978**). "Evaluation of mutual radiation impedances between circular pistons by impulse response and asymptotic methods," J. Sound Vib. **59**(2), 221–235.
Struve, H. (**1882**). "Beitrag zur Theorie der Diffraction an Fernröhren" ("Contribution to the theory of diffraction on telescopes"), Ann. Phys. **253**(2), 1008–1016.
Valier-Brasier, T. (**2017**). "Rayonnement acoustique" ("Acoustic radiation"), http://www.dalembert.upmc.fr/home/valier-brasier/images/cours/Poly_Rayonnement_1718.pdf. (Last viewed May 9, 2022).
Van Buren, A. L., and King, B. J. (**1973**). "Self and mutual acoustic radiation impedances for two coplanar unbaffled disks," J. Sound Vib. **26**(1), 29–40.
Wallace, C. E. (**1972**). "Radiation resistance of a rectangular panel," J. Acoust. Soc. Am. **51**(3B), 946–952.
Watson, G. (**1966**). *A Treatise on the Theory of Bessel Functions*, 2nd ed. (Cambridge University Press, Cambridge, UK).
Williams, E. G. (**1999**). *Fourier Acoustics Sound Radiation and Nearfield Acoustical Holography* (Academic Press, New York).
Wu, H., Jiang, W., Zhang, Y., and Lu, W. (**2014**). "A method to compute the radiated sound power based on mapped acoustic radiation modes," J. Acoust. Soc. Am. **135**(2), 679–692.
Zwillinger, D., Moll, V., Gradshteyn, I. S., and Ryzhik, I. M. (**2014**). *Table of Integrals, Series, and Products* (Academic Press, Boston, MA).